Gramicidin Cation Channel: An Experimental Determination of the Right-Handed Helix Sense and Verification of β-Type Hydrogen Bonding†

L. K. Nicholson and T. A. Cross*

Department of Chemistry and Institute of Molecular Biophysics, Florida State University, Tallahassee, Florida 32306-3006

Received July 31, 1989; Revised Manuscript Received September 18, 1989

ABSTRACT: Due to the difficulty of obtaining protein/lipid cocrystals for diffraction studies, structural research on intrinsic membrane proteins and polypeptides has been largely restricted to indirect experimental techniques. Hence, many fundamental questions associated with peptide/lipid systems remain unanswered. In particular, the handedness of the gramicidin A transmembrane ion channel incorporated into lipid bilayers has been an open question for nearly two decades. In this study, solid-state ^{15}N NMR spectroscopy is employed to probe directly the secondary structure of the polypeptide backbone. Recent determinations of the ^{15}N chemical shift anisotropy tensor with respect to the molecular frame enable the quantitative evaluation of the ^{15}N chemical shift resonances obtained from oriented dimyristoylphosphatidylcholine (DMPC) bilayer samples containing specific site ^{15}N labeled gramicidin. This direct structural approach verifies the β-sheet hydrogen-bonding pattern proposed by Urry [Urry, D. W. (1971) *Proc. Natl. Acad. Sci. U.S.A. 68*, 672–676] and determines that in our DMPC bilayer preparations the gramicidin channel is right-handed. Additional structural information is provided by the ^{15}N chemical shift data in the form of orientational constraints on the C_α–C_α axis orientation of individual peptides relative to the helix axis. The significance of these solid-state NMR results lies in the direct determination of the helix sense and the verification of the β-type hydrogen bonding, in the development of the solid-state NMR methods for obtaining such information, and in emphasizing the importance of having direct structural data at atomic resolution.

Direct structural information from spectroscopic or scattering analyses is essential for solving fundamental questions associated with the structure and dynamics of macromolecules. The generally accepted structural model of the gramicidin A transmembrane ion channel incorporated into lipid systems has been supported by a substantial literature of indirect structural evidence such as the interpretation of isotropic chemical shifts in solution NMR experiments and molar ellipticity in circular dichroism experiments. For intrinsic membrane proteins and polypeptides, obtaining direct structural information has been particularly challenging because of the difficulty in crystallizing such polypeptide/lipid systems for diffraction studies. With the advent of efficient solid-phase peptide synthesis and effective approaches for orienting lipid bilayers, solid-state NMR techniques can now be applied to elucidate the atomic resolution structure of intrinsic membrane polypeptides, eliminating the need to rely on indirect methods.

This paper presents direct structural data achieved by solid-state NMR of single site ^{15}N labeled gramicidin in oriented lipid bilayers. Quantitative interpretation of the ^{15}N chemical shifts has been made possible by a recent determination of the chemical shift tensor orientation for specific sites in gramicidin (Teng & Cross, 1989) as well as for appropriate model compounds (Oas et al., 1987; Hartzell et al., 1987). In the work presented here, atomic resolution detail is derived from the ^{15}N resonances of the Val_1–Val_7 sites by providing orientational constraints that are uniquely consistent with a right-handed helix. Although the β-sheet pattern of hydrogen bonding proposed by Urry (1971) is confirmed by this solid-state ^{15}N NMR study, the previously accepted left-handed sense of the helical channel (Urry et al., 1982; Urry, 1985) is shown to be incorrect in extended bilayer systems.

In solid-state NMR spectroscopy the orientation dependence of nuclear spin interactions, such as the chemical shift anisotropy (CSA), is retained and is represented by a second-rank Hermitian tensor. Diagonalization of the CSA tensor yields the principal components of the interaction, $\sigma_{11} < \sigma_{22} < \sigma_{33}$. These principal components comprise an orthogonal coordinate system denoted the principal axis system (PAS). The CSA tensor can be viewed as an ellipsoid having a fixed orientation with respect to the molecular frame, with the PAS of this tensor coincident with the principal axes of the ellipsoid. For a given orientation of the nuclear site relative to the magnetic field, only the component of the CSA tensor in the direction of the field is detected, resulting in a single observed chemical shift given by

$$\sigma_{obs} = \sigma_{11} \cos^2 \theta_{11} + \sigma_{22} \cos^2 \theta_{22} + \sigma_{33} \cos^2 \theta_{33}$$

where σ_{ii} represents the principal values of the CSA tensor and θ_{ii} the angle between the ith principal axis and the direction of the applied magnetic field ($i = 1$–3). The $\cos^2 \theta_{ii}$ are the direction cosines expressing the orientation of the PAS with respect to the laboratory fixed coordinate system, and their sum is unity. Since the orientation of the PAS is known relative to the molecular frame for specific sites in the gramicidin molecule, the chemical shift interaction provides an opportunity for obtaining atomic resolution details concerning the structure and dynamics of this widely studied ion-transport channel.

Lipid bilayer systems have a distinct advantage for study by solid-state NMR because the planar bilayers can be uniformly aligned parallel to one another. The gramicidin channel lies within the hydrocarbon domain of the bilayer, with the channel axis parallel to the bilayer normal (Nicholson et al., 1987; Smith & Cornell, 1986). Thus, alignment of the bilayers results in uniform orientation of the gramicidin channels. ^{15}N-Labeled gramicidin oriented with the channel axis parallel

† The NMR spectrometer used in this study was purchased with the aid of NSF Grant DMB-8504250. This work is supported by NIH Grant AI-23007 and NSF Grant DMB-8451876 with the Procter and Gamble Co. through a Presidential Young Investigator Award to T.A.C. Support provided through an Alfred P. Sloan Research Fellowship to T.A.C. is also greatly appreciated.

0006-2960/89/0428-9379$01.50/0

to the static magnetic field gives rise to a single sharp resonance for each unique site, corresponding to the average orientation of the CSA tensor with respect to the magnetic field. The frequency of this resonance, along with knowledge of the orientation of the CSA tensor in the molecular frame, allows the determination of the orientation of the peptide plane relative to the channel axis.

The β-helix was originally described by Urry (1971) as a model for the gramicidin channel as well as other polypeptides with strictly alternating L and D amino acid sequences. This model consists of a strand of polypeptide chain wound into a helical motif, stabilized by intramolecular hydrogen bonds exhibiting the same hydrogen-bonding pattern as found in a parallel β-pleated sheet. Two of these helices associate head (amino terminus)-to-head to form a dimer that spans the bilayer, with the monomer–monomer junction formed by six intermolecular hydrogen bonds in an antiparallel β-pleated sheet pattern. In each monomer, the hydrogen-bonding scheme results in the plane of the peptide linkages being approximately parallel to the helix axis, thereby optimizing hydrogen bonding in the polypeptide backbone. In the standard β-pleated sheet secondary structure the peptide planes alternate orientations, with the faces of adjacent planes lying on opposite sides of the sheet. Consequently, the β-type hydrogen bonding in this model requires that the C–O bond vectors for adjacent peptide linkages alternate between being parallel and antiparallel to the helix axis. Here the helix axis is defined as a vector parallel to the global rotational axis of the channel (Nicholson et al., 1987; Cornell et al., 1988; Fields et al., 1988) originating at the N-terminus and pointing toward the C-terminus. This type of hdyrogen bonding is distinct from that of an α-helix, where the C–O bond vectors are all parallel to the helix axis. Consequently, while an α-helix is characterized by a rise per single amino acid residue, the characteristic repeating unit in a β-helix is a dipeptide.

Figure 1 shows model structures of left- and right-handed β-helices. It can be seen that the C_α–C_β bond vectors are approximately radial to the helix axis, while the C_α–H bond vectors are axially oriented. The requirement for strict alternation between L and D stereochemistry of the amino acid sequence of a β-helix is apparent, since replacement of an L residue with a D residue exchanges the C_α–C_β and C_α–H bond vectors, resulting in steric crowding of the side chain by the next turn of the helix. Although both left-handed and right-handed β-helix models are energetically reasonable, differing by approximately 2 kcal/mol (Venkatachalam & Urry, 1983), there are substantial structural differences between these models. The radial orientation of the C_α–C_β bond vectors for a right-handed β-helix is achieved only when the C–O bond vectors of L residues point toward the N-terminus and the C–O bond vectors of D residues point toward the C-terminus of the helix (Koeppe & Kimura, 1984). For a left-handed version, the orientations of the L and D C–O bond vectors are reversed. Similarly, while in a left-handed helix the N–H bond vectors of L residues are parallel to the helix axis, they are antiparallel in the right-handed helix. Consequently, the direction of the peptide planes relative to the helix axis provides a clear distinction between right- and left-handed versions of the channel. Therefore, if the orientation of individual peptide planes within the backbone of the gramicidin channel can be determined, the handedness of the helix can be elucidated.

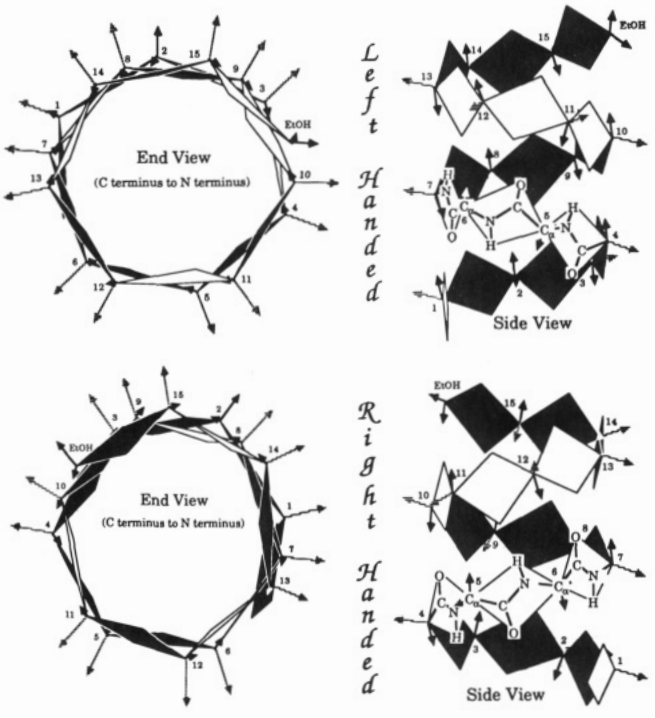

FIGURE 1: Model structures of left- and right-handed β-helices highlighting the orientation of the peptide planes. The shaded side of each peptide plane faces toward the helix axis. Broken arrows represent the C_α–C_β bond orientations; solid arrows represent the C_α–H bond orientations. Only a single monomer is shown of the channel-forming dimer. To avoid steric hindrances between side chains and the next turn of the helix, the N–H bond vectors of L residues must be antiparallel to the helix axis in the right-handed version and parallel in the left-handed version. The coordinates used to generate these model structures were generously provided by Eric Jakobsson, See-Wing Chiu, and Matthew Brenneman of the University of Illinois.

Materials and Methods

Sample Preparation. ^{15}N-Labeled residues were incorporated specifically at the Val_1, Gly_2, Ala_3, Leu_4, Ala_5, Val_6, or Val_7 position of gramicidin via solid-phase peptide synthesis as previously described (Fields et al., 1988, 1989). Dimyristoylphosphatidylcholine (DMPC) was purchased from Sigma Chemical Co. and was used without further purification. Spectroanalyzed benzene was purchased from Fisher Chemical Co., TFE (99+%) was purchased from Aldrich Chemical Co., and ethanol (absolute) was purchased from Midwest Grain Products. The solvent systems used in this study have been shown to yield a polypeptide backbone conformation identical with the gramicidin channel conformation (LoGrasso et al., 1988; Moll & Cross, 1989). Powder pattern samples were prepared by codissolving 55 mg of specific site ^{15}N-labeled gramicidin with 165 mg of DMPC in 50 mL of either TFE or 5% ethanol in benzene. The solution was rotatory evaporated to a thin film and placed under vacuum overnight to completely remove the solvent. The dry powder was loaded into a glass sample holder and sealed. Uniformly aligned samples were prepared by using the following technique. Nine milligrams of specific site ^{15}N labeled gramicidin was codissolved with 26 mg of DMPC in 300 μL of 5% ethanol in benzene and placed in the freezer overnight. After thawing at room temperature, the solution was immediately spread in equal aliquots with a micropipet onto 30 clean glass cover slips (Corning Glass Co.), 12 mm × 5.7 mm, and allowed to evaporate to a thin film under ambient conditions. The plates were then placed under vacuum overnight to ensure complete removal of the solvent. Upon removal from the vacuum, 0.5 μL of HPLC grade H_2O was added to each cover slip, and the cover slips were immediately stacked in the sample holder to minimize evaporation. The sample holder was constructed from a 13 mm long piece of 8 mm square glass tubing

(Wilmad Glass Co.), and glass endcaps were cut from a microscope slide. An endcap was fixed with quick-setting epoxy to one end of the tube prior to loading. When all 30 cover slips had been loaded, the sample was further hydrated to 30% and the second endcap sealed in place with epoxy. After the epoxy was allowed to cure thoroughly at room temperature (approximately 12 h), the sample was placed in an incubator at 45 °C for a minimum of 2 weeks, during which time uniform hydration and alignment evolved.

NMR Experiments. The ^{15}N NMR experiments were performed on a modified narrow bore IBM/Bruker WP200 NMR spectrometer with a solids package. A home-built static (i.e., non magic angle spinning) probe equipped with variable-temperature control was used for acquisition of data from both randomly dispersed and uniformly aligned samples. Cross polarization between the abundant ^1H pool and the rare ^{15}N nuclei was used with a Hahn echo to minimize probe ringing. The following pulse sequence parameters were employed: 5-μs 90° pulse length; 1-ms mixing/spin lock period; 48-μs echo delay, 62.5-kHz sweep width; and 7-s recycle delay. The number of scans accumulated for each spectrum is given in the corresponding figure legend.

Computer Calculations. Although a unique orientation of a peptide plane cannot be determined from the ^{15}N chemical shift frequency due to the $\sigma_{ii} \cos^2 \theta_{ii}$ dependence of the interaction, the range of possible orientations corresponding to this frequency can be calculated. For individual peptide planes, chemical shifts corresponding to a series of peptide plane orientations were calculated and compared to the experimentally observed chemical shift.

To maintain the integrity of a β-helix, flexibility and motions in the polypeptide backbone are largely restricted to a librational motion described as occurring about an axis joining adjacent α carbons. The peptide plane can undergo an almost pure rotation about this axis since the C_α^{i-1}–C_1^{i-1} and the N^i–C_α^i bonds are nearly parallel, allowing a crankshaft-type rocking of the linkage. Furthermore, the orientation of this axis is restricted, since the combined C_α–C_α tilts of a dipeptide must have a positive component in the helix axis direction if the polypeptide is to form a helix. For a fixed orientation of the C_α–C_α axis of a given peptide linkage, rotation through 360° about this axis will yield all possible orientations of the peptide plane for a given folding motif of the backbone. Therefore, the C_α–C_α axis is chosen as a convenient axis about which the chemical shift tensor may be rotated to investigated the possible orientations of each peptide plane.

Before the calculations are made, the relative orientation of the ^{15}N CSA tensor and the molecular frame must be known. This has been achieved for the Ala_3 and Leu_4 sites in the gramicidin molecule by simulation of the $^{13}C_1$ dipolar broadened ^{15}N static chemical shift powder patterns. This approach locates the C_1–N bond relative to the PAS of the ^{15}N CSA tensor and, combined with the model compound result that σ_{22} is perpendicular to the peptide plane, results in location of the ^{15}N CSA tensor relative to the molecular frame. The orientation of this tensor with respect to the peptide plane is very similar for the Ala_3 and Leu_4 sites, with $\alpha = 0°$ and $\beta = 104°$ for the Ala_3 site and $\alpha = 0°$ and $\beta = 105°$ for the Leu_4 site (Teng & Cross, 1989). As an approximation for interpretation of the ^{15}N chemical shift data, it is assumed that the orientation of the ^{15}N CSA tensor relative to the molecular frame is similar for the Val_1, Gly_2, Ala_5, Val_6, and Val_7 sites, with $\alpha = 0°$ and $\beta = 105°$. Although the exact orientation of these tensors in the peptide plane may vary somewhat, the variation is not expected to be substantial (Oas et al., 1987).

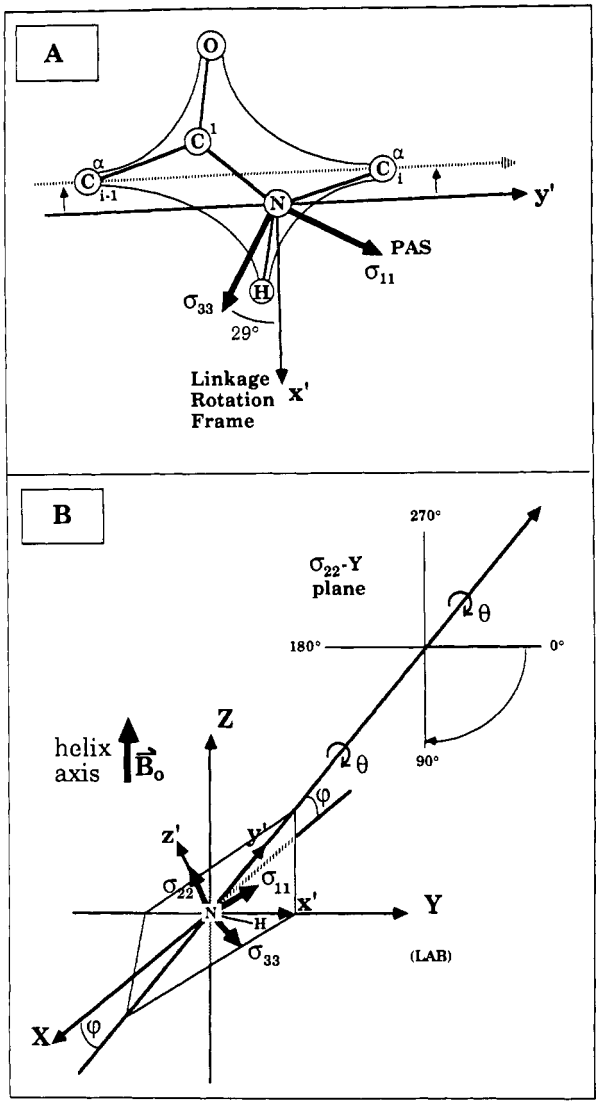

FIGURE 2: (A) Location of the principal axis system (PAS) of the ^{15}N chemical shift tensor in the peptide plane. The orientation shown corresponds to $\alpha = 0°$ and $\beta = 105°$. The linkage rotation frame (x', y', z') is defined as shown, with y' pointing along the C_α–C_α axis in the positive chain direction (N- to C-terminus), x' in the pepide plane as shown, and z' orthogonal to x' and y'. Although the ^{15}N nucleus does not lie on the C_α–C_α axis, the origin of the PAS can be translated onto this axis for the purposes of calculation, since rotations are invariant under translation. (B) Linkage rotation frame shown in its initial position relative to the laboratory fixed reference frame (X, Y, Z). The y' axis is placed for convenience in the XZ plane at some angle of inclination φ above the XY plane, corresponding to the angle of tilt of the C_α–C_α axis. The x' axis is initially placed coincident with Y. Rotation about y' by θ in a positive sense defined by the right-hand rule will first bring the N–H bond vector approximately antiparallel to the helix axis at $\theta = 90°$ and then parallel to the helix axis at $\theta = 270°$. Rotation of the peptide plane through 360° about y' will generate all possible orientations of the ^{15}N chemical shift tensor for a given backbone folding motif.

Calculation of the observed ^{15}N chemical shift as a function of peptide plane rotation is done through a series of unitary transformations from the principal axis system (PAS) of the CSA tensor to the laboratory-fixed reference frame. Initially, the PAS frame is expressed in the molecular frame via a transformation using the Euler angles α and β. The molecule frame representation of the CSA tensor is then transformed to the linkage rotation frame (x', y', z') defined in Figure 2A by using the peptide plane geometry given in Momany et al. (1975). The linkage rotation frame is then set in an initial position relative to the laboratory fixed reference frame (X,

Table I: Chemical Shift Values Obtained from Specific Sites in the Gramicidin Molecule

site	σ_{iso}[a]	σ_{11}[b]	σ_{22}[b]	σ_{33}[b]	σ_{obs}[a]
Val_1	104 ± 3	−59 ± 3	−41 ± 3	100 ± 3	198 ± 1
Gly_2	90	−68	−39	107	113
Ala_3	105	−65	−39	104	198
Leu_4	98	−65	−34	99	145
Ala_5	104	−66	−37	103	198
Val_6	99	−62	−37	103	145
Val_7	100	−63	−40	103	196

[a] Chemical shifts in parts per million relative to a saturated aqueous solution of $^{15}NH_4NO_3$. [b] Chemical shifts in parts per million relative to $\sigma_{iso} = 0$.

Y, *Z*) as shown in Figure 2B. If the magnetic field B_0 is chosen to be in the *Z* direction, the position of the CSA tensor in the *XY* plane is arbitrary and the *y'* axis can be placed for convenience in the *XZ* plane at some angle of inclination, φ, with *x'* coincident with *Y*. The peptide plane is then rotated in increments of 0.5° about the *y'* axis through 360° by using the Euler parameters technique that, with a single transformation matrix, allows rotation of a body about an axis which is fixed relative to both the body and the stationary laboratory frame. Since the static magnetic field is chosen to be in the *Z* direction, the observed chemical shift for each incremental rotation is the (33) component of the corresponding laboratory representation of the chemical shift tensor. In summary, an orientation of the C_α–C_α axis is first assumed, the chemical shift tensor is rotated about this axis through 360°, and the chemical shift is calculated as a function of θ.

Results

The principal components of the ^{15}N CSA tensor for each isotopically labeled site were determined by recording the static powder pattern spectrum and simulating the resulting line shape. Examples of such a determination in the gramicidin backbone have been published (Teng & Cross, 1989). Static powder patterns were obtained from randomly dispersed samples of a dry mixture of specific site ^{15}N labeled gramicidin and DMPC. The principal components of the CSA tensor for each site are summarized in Table I, with the chemical shift frequencies given relative to σ_{iso}. The frequency of σ_{iso} for each site is also given in Table I relative to a saturated aqueous solution of $^{15}NH_4NO_3$.

Figure 3 shows ^{15}N NMR spectra obtained from uniformly aligned samples positioned in the magnet such that the bilayer normal is parallel with the static magnetic field. These spectra were recorded at room temperature (28 °C), which is above the transition temperature at which global rotational motions become rapid on the NMR time scale (Nicholson et al., 1987). These spectra represent single site ^{15}N labeled gramicidins; consequently, the assignment of the resonance to a specific nuclear site in the molecule is trivial. From these spectra it is clear that our samples have a single backbone conformation, since a single narrow resonance is observed for each site. Furthermore, this backbone conformation is that of the channel, since these samples prepared from benzene/ethanol solution yield ^{15}N resonances that are identical with those obtained from samples prepared from organic solvents which have been shown to yield the channel backbone conformation (LoGrasso et al., 1988; Killian et al., 1988; Fields et al., 1988; Nicholson et al., 1989). It can also be seen that an alternating pattern of chemical shift frequencies occurs along the polypeptide backbone in the N-terminal region studied here. The odd-numbered (L) residues yield shifts at frequencies closer to σ_{33} than the even-numbered (D) residues. The observed chemical shift for the Val_1, Ala_3, and Ala_5 sites is 198 ppm,

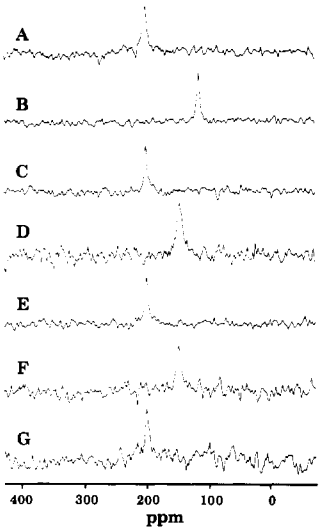

FIGURE 3: Solid-state ^{15}N NMR spectra obtained from oriented bilayer samples containing specific site ^{15}N labeled gramicidin A. Chemical shifts are given relative to a saturated aqueous solution of $^{15}NH_4NO_3$. The samples were placed in the magnet such that the bilayer normal was parallel to the field. All spectra were recorded at 28 °C. (A) [^{15}N]Val_1-gramicidin A, 23 480 scans. (B) [^{15}N]Gly_2-gramicidin A, 12 072 scans. (C) [^{15}N]Ala_3-gramicidin A, 12 212 scans. (D) [^{15}N]Leu_4-gramicidin A, 8000 scans. (E) [^{15}N]Ala_5-gramicidin A, 13 556 scans. (F) [^{15}N]Val_6-gramicidin A, 15 484 scans. (G) [^{15}N]Val_7-gramicidin A, 10 000 scans.

and for Val_7 it is 196 ppm. The Gly_2, Leu_4, and Val_6 sites yield resonances at 114, 145, and 145 ppm, respectively. These values are given relative to the reference and are listed in Table I.

The handedness of the helix formed by the gramicidin channel can be determined from the structural constraints imposed by the observed chemical shift of the oriented single site labeled samples. The same constraints can also be used to verify a β-type hydrogen-bonding pattern for the backbone of gramicidin solubilized in a lipid bilayer. Such hydrogen bonding has recently been shown for two nonchannel conformations of gramicidin in the absence of lipids by X-ray diffraction of gramicidin crystals prepared from organic solutions (Langs, 1988; Wallace & Ravikumar, 1988).

To interpret the ^{15}N chemical shift data in terms of structure, the orientation of the CSA tensor with respect to the peptide plane and the orientation of the helix axis with respect to the applied magnetic field have been established. In addition, it must be ascertained that the chemical shift differences observed in Figure 3 are due to structural differences rather than differences in local dynamics. The ^{15}N chemical shift spectrum of single site ^{15}N labeled gramicidin obtained from an oriented bilayer sample reflects the motionally averaged orientation of the associated CSA tensor relative to the magnetic field. When the axis of global rotation is placed parallel to the field, the observed chemical shift is unaffected by this rotation, since all orientations about this axis give rise to the same chemical shift. However, local motions of the peptide backbone that affect the orientation of the CSA tensor with respect to the field will average the tensor (Nicholson et al., 1989). For the Val_1, Ala_3, Ala_5, and Val_7 sites it is clear that any local motions which may exist do not extensively average the σ_{33} tensor element, since the observed chemical shift is so close to that of the static σ_{33} value. The amplitude of these local motions has recently been shown to be similar for both odd- and even-numbered sites (Nicholson et al., 1989). Consequently, the variation in chemical shift seen in Figure 3 is not the result of dynamic variation. Furthermore, variation

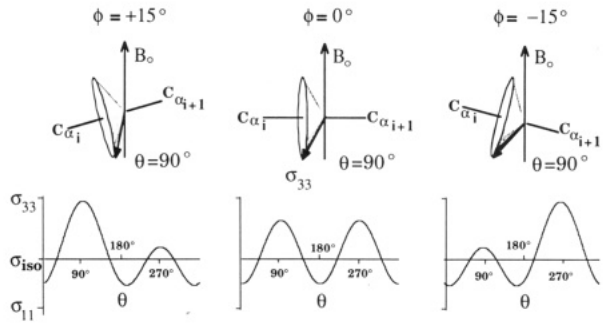

FIGURE 4: Chemical shift as a function of motional axis orientation. Three orientations of the C_α–C_α axis relative to the static magnetic field (B_0) and the corresponding σ_{obs} vs θ plots. Only σ_{33} and its cone of revolution are shown for clarity. This illustrates that equal but opposite C_α–C_α axis orientations relative to the XY plane ($\varphi = \pm 15°$) yield plots that are phase shifted by 180° with respect to θ and that a symmetric plot is obtained only when the C_α–C_α axis lies in the XY plane ($\varphi = 0°$). This asymmetry about the C_α–C_α axis enables the unique location of the peptide plane relative to the helix axis, elucidating the right-handed sense of the gramicidin channel.

in the orientation of the CSA tensor with respect to the molecular frame has been shown to be small. Therefore, the different ^{15}N chemical shift frequencies observed for the odd and even sites shown in Figure 3 result directly from differences in the orientation of individual peptide planes with respect to the helix axis.

Figure 4 shows three different orientations of the C_α–C_α axis with respect to the magnetic field, $\varphi = +15°$, 0°, and −15°. For each of the three orientations, the corresponding plot of σ_{obs} versus θ is shown. For clarity and because of its primary influence on the observed chemical shift of the ^{15}N sites in gramicidin, only σ_{33} and its cone of revolution are shown in this figure. However, the plots of σ_{obs} vs θ were generated with the full tensor as described above. These plots illustrate that equal but opposite values of φ yield plots that are 180° out of phase with respect to θ and that only when the C_α–C_α axis lies in the XY plane ($\varphi = 0°$) is the plot of σ_{obs} vs θ symmetric about $\theta = 180°$. In general, because the axis about which the peptide plane is rotated does not coincide to any of the three principal axes of the CSA tensor, the chemical shift is not symmetric about this axis. Specifically, for $\varphi = +15°$ the chemical shift is very different at $\theta = 90°$ and $\theta = 270°$, corresponding to the N–H bond vector being approximately antiparallel and parallel to the helix axis, respectively. It is this feature of the ^{15}N CSA tensor located within the peptide plane that yields important and conclusive results concerning the handedness of the helix.

In a β-helix, the orientation of the C_α–C_α axis is restricted by the helical pitch, since the C_α–C_α tilts of two adjacent peptide planes must result in a positive projection of the dipeptide along the helix axis equal to the rise per dipeptide. Structural constraints on the dihedral angles require a positive value of φ for each peptide plane, although the degree of C_α–C_α tilt is expected to alternate between large and small values due to the alternation of peptide plane orientations in the β-helix. Given the required positive value for φ and hence the asymmetric nature of the σ_{obs} vs θ plot, an alternating nature of observed chemical shifts would be expected for a β-helical folding motif of the gramicidin backbone. This alternating nature is indeed observed, as was shown in Figure 3 and Table I. For the L sites, which include Val_1, Ala_3, and Val_7, the observed chemical shift ranges between 196 and 198 ppm. This requires θ to be in the vicinity of 90°, which corresponds to the N–H bond vector of the amide group pointing in an antiparallel direction relative to the helix axis. This unambiguous result determines the helix as being *right-handed*. The D sites, Gly_2, Leu_4, and Val_6, have chemical shifts that range from 113 to 145 ppm, which is consistent with an approximate θ orientation of 270°. This 180° rotation of the peptide plane for alternate peptide linkages verifies of β-helical hydrogen-bonding pattern of the Urry model. If the helix were left-handed, the alternating nature would be reversed, with D residues yielding chemical shifts close to σ_{33} and the L sites resonances well removed from σ_{33}.

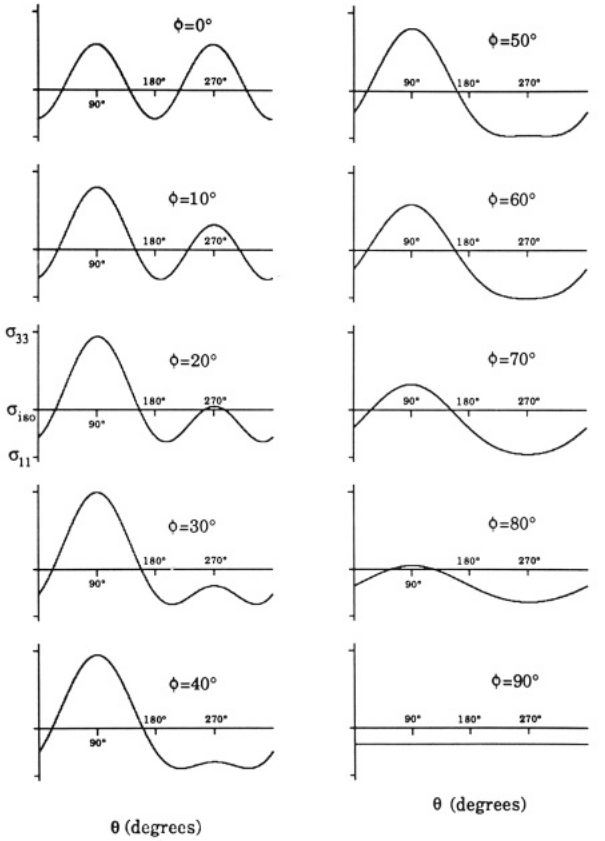

FIGURE 5: Calculated σ_{obs} vs θ for 10° increments of C_α–C_α axis orientation as defined by φ. Different local maxima occur at $\theta = 90°$ and $\theta = 270°$, the magnitude of which is strongly dependent on φ. The absolute maximum of σ_{33} is encountered at $\theta = 90°$ when $\varphi = 30°$, corresponding to the orientation that places the σ_{33} component of the chemical shift tensor directly antiparallel to B_0. The range of possible C_α–C_α axis orientations for a given peptide linkage can be determined by comparing the variation in the local maximum chemical shift, σ_{max}, at $\theta = 90°$ for L residues and at $\theta = 270°$ for D residues as a function of φ to the experimentally obtained σ_{obs}. The resulting range is $15° < \varphi < 45°$ for the peptide planes containing the Val_1, Ala_3, Ala_5, and Val_7 N–H bonds, $0° < \varphi < 7°$ for the peptide planes containing the Leu_4 and Val_6 N–H bonds, and $0° < \varphi < 14°$ for the peptide plane containing the Gly_2N–H bond.

In addition to these results, the ^{15}N chemical shift data can be used to place limits on the orientation of the C_α–C_α axis for each individual peptide linkage. As the CSA tensor is rotated about a given C_α–C_α axis orientation, the observed chemical shift traces out a line on the surface of the chemical shift ellipsoid. Depending upon the orientation of the C_α–C_α axis, different local maxima and minima are encountered. Figure 5 shows σ_{obs} vs θ for a number of C_α–C_α axis orientations, illustrating the dependence of σ_{max} on φ. Local maxima occur at 90° and 270°, the magnitude of which is strongly dependent on φ. The local maxima at 90° apply to the L residues, since they have been shown above to lie in this region of θ, while local maxima at 270° apply to the D residues. The variation in the local maximum chemical shift, σ_{max}, as a function of φ may be used to place limits on the possible range

of C_α–C_α axis orientations. The observed chemical shifts for the L residues of 196–198 ppm result in a range of possible C_α–C_α axis orientations of $15° < \varphi < 45°$. Similarly, the observed chemical shift for the Leu_4 and Val_6 sites of 145 ppm results in a range of possible C_α–C_α axis orientations of $0° < \varphi < 7°$. Finally, the chemical shift of 113 ppm obtained from the Gly_2 site places limits of $0° < \varphi < 14°$ for the C_α–C_α tilt of this peptide plane.

Discussion

Many indirect structural analysis techniques have been applied to the study of the gramicidin transmembrane channel and have led to the general acceptance of the $\beta^{6.3}$-helix model. This model for the gramicidin channel was originally based upon circular dichroism, solution NMR studies in organic solvents, and conformational analysis (Urry, 1971). Since then it has been shown that the structure is highly variable in organic solvents, where double-stranded forms of a gramicidin dimer frequently dominate. Obtaining structural data in a lipid environment has been considerably more difficult. The CD results are dependent upon low light scattering, and the spectra obtained are profoundly complicated by the presence of four indole side chains. Weinstein et al. (1979) showed that only the carboxy terminus was exposed to the aqueous solution when gramicidin was incorporated into vesicles. These results suggested that, in fact, the channel was a single-stranded dimer with the amino terminus in the bilayer center. Many other studies have provided additional evidence that the channel conformation is indeed a head-to-head dimner of a single-stranded β-helix.

Evidence for the helix sense has been even more indirect. Urry's study of isotropic ^{13}C chemical shifts of carbonyl carbons in the presence of Tl^+, Ba^{2+}, and Na^+ appeared to be consistent with a specific left-handed model described in his paper (Urry et al., 1982). The interpretation of isotropic chemical shifts is complicated because it is the interpretation of an average effect, rather than a detailed analysis of the chemical shift tensor. In the presence of various ions, how is the chemical shift tensor affected? Are both magnitude and orientation affected for these ^{13}C carbonyl carbon sites? The isotropic chemical shift studies were performed at 70 °C on solutions of gramicidin packaged in monoacyl lecithins (lyso-PC). Both the structural and functional states of gramicidin appear to be highly sensitive to their environment. Structural studies on gramicidin in nonpolar solvents have been performed to simulate the hydrocarbon domain of a lipid bilayer. Veatch et al. (1974) found that, on the basis of CD, ^1H NMR, and IR spectroscopies, an equilibrium exists between four different conformational species in a single nonpolar solvent system and postulated a family of interconverting double-stranded helices to account for their observations. One- and two-dimensional ^1H, ^{13}C, and ^{15}N NMR spectra of gramicidin in DMSO were found to be consistent with a rapid interconversion between ordered and disordered states in equilibrium, where the ordered state is described as a single-stranded, left-handed β-helix (Hawkes et al., 1987). Furthermore, the functional state of gramicidin in diacyl phospholipids exhibits a solvent history dependence (Killian et al., 1988; LoGrasso et al., 1988). Therefore, the sensitivity of gramicidin to its environment makes comparison of structural interpretations in different lipid systems difficult. Whether or not the conformation in lyso-PC is the same channel backbone conformation as shown to be present in our DMPC bilayer preparations is an open question. It is possible that Urry's preparations do indeed contain the left-handed helix, while our samples of gramicidin in extended DMPC bilayers are clearly shown to contain only a right-handed β-helix.

This is not the first time that experimental evidence has been put forth for a right-handed helix. Two-dimensional ^1H NMR spectra of gramicidin incorporated into SDS micelles have been interpreted to show that in this detergent environment the gramicidin conformation is a head-to-head, single-stranded, right-handed β-helix (Arseniev et al., 1985). More recently, anomolously broad lines in solid-state ^{13}C NMR spectra of oriented samples have prompted the interpretation that a mixture of gramicidin conformations, possibly including a mixture of right- and left-handed helices, may exist in extended bilayer preparations of DMPC (Cornell et al., 1988). Given the resolution (average line widths of 5 ppm) and the observed chemical shift differences between L and D amino acids (50 ppm) in our ^{15}N NMR experiments, it is not possible to interpret our results as a mixture of left- and right-handed helices. If both forms were present, two well-resolved resonances would be observed for each individual site in an oriented sample corresponding to the peptide plane being either parallel or antiparallel to the helix axis.

The results presented here clearly demonstrate that, in the DMPC bilayer preparations used, a single conformational state is evident from the sharp line spectra of the many single sites studied, that a right-handed helix is formed, and that β-type hydrogen bonding is verified. This determination is independent of the structural model details and is only dependent on the general steric hindrances encountered in folding the backbone into a helix. Additional structural information is provided in the form of orientational constraints for the C_α–C_α axis of adjacent residues. The significance of these solid-state NMR results lies both in the determination of the helix sense and in the verification of the β-type hydrogen bonding and reaffirms the importance of obtaining direct structural evidence for eliminating potential structural models from consideration. The application of solid-state NMR techniques using oriented samples has the potential not only for providing general information about the folding pattern but also for determining the specific torsion angles in the polypeptide backbone (Cross & Opella, 1985; Cross, 1986; Opella et al., 1987). Such detailed studies of gramicidin utilizing the same single site labeled molecules used here are underway.

Acknowledgments

We are deeply indebted to Richard Rosanske and Thomas Gedris for their skillful maintenance, modification, and repair of the NMR facility. We deeply appreciate Eric Jakobsson, See-Wing Chiu, and Matthew Brenneman at the University of Illinois for providing the coordinates for the right- and left-handed gramicidin helices.

Registry No. DMPC, 18194-24-6; gramicidin A, 11029-61-1.

References

Arseniev, A. S., Barsukov, I. L., Bystrov, V. F., Lomize, A. L., & Ovchinnikov, Yu. A. (1985) *FEBS Lett. 186*, 168–174.

Cornell, B. A., Separovic, F., Baldassi, A. J., & Smith, R. (1988) *Biophys. J. 53*, 67–76.

Cross, T. A. (1986) *Biophys. J. 49*, 124–126.

Cross, T. A., & Opella, S. J. (1985) *J. Mol. Biol. 182*, 367–381.

Fields, C. G., Fields, G. B., Noble, R. L., & Cross, T. A. (1989) *Int. J. Pept. Protein Res. 33*, 298–303.

Fields, G. B., Fields, C. G., Petefish, J., Van Wart, H. E., & Cross, T. A. (1988) *Proc. Natl. Acad. Sci. U.S.A. 85*, 1384–1388.

Hartzell, C. J., Whitfield, M., Oas, T. G., & Drobny, G. P. (1987) *J. Am. Chem. Soc. 109*, 5966–5969.
Hawkes, G. E., Lian, L.-Y., Randall, E. W., Sales, K. D., & Curzon, E. H. (1987) *Eur. J. Biochem. 166*, 437–445.
Killian, J. A., Prasad, K. U., Hains, D., & Urry, D. W. (1988) *Biochemistry 27*, 4848–4855.
Koeppe, R. E., II, & Kimura, M. (1984) *Biopolymers 23*, 23–38.
Langs, D. A. (1988) *Science 241*, 188–191.
LoGrasso, P. V., Moll, F., III, & Cross, T. A. (1988) *Biophys. J. 54*, 259–267.
Moll, F., III, & Cross, T. A. *Biophys. J.* (in press).
Momany, F. A., McGuire, R. F., Burgess, A. W., & Sheraga, H. A. (1975) *J. Phys. Chem. 79*, 2361–2381.
Nicholson, L. K., Moll, F., III, Mixon, T. E., LoGrasso, P. V., Lay, J. C., & Cross, T. A. (1987) *Biochemistry 26*, 6621–6626.
Nicholson, L. K., LoGrasso, P. V., & Cross, T. A. (1989) *J. Am. Chem. Soc. 111*, 400–401.
Oas, T. G., Hartzell, C. J., Dahlquist, F. W., & Drobny, G. P. (1987) *J. Am. Chem. Soc. 109*, 5962–5966.
Opella, S. J., Stewart, P. L., & Valentine, K. G. (1987) *Q. Rev. Biophys. 19*, 7–49.
Smith, R., & Cornell, B. A. (1986) *Biophys. J. 49*, 117–118.
Teng, Q., & Cross, T. A. (1989) *J. Magn. Reson.* (in press).
Urry, D. W. (1971) *Proc. Natl. Acad. Sci. U.S.A. 68*, 672–676.
Urry, D. W. (1985) *Enzymes Biol. Membr. (2nd Ed.) 1*, 229–257.
Urry, D. W., Goodall, M. C., Glickson, J. D., & Mayers, D. F. (1971) *Proc. Natl. Acad. Sci. U.S.A. 68*, 1907–1911.
Urry, D. W., Walker, J. T., & Trapane, T. L. (1982) *J. Membr. Biol. 69*, 225–231.
Veatch, W. R., Fossel, E. T., & Blout, E. R. (1974) *Biochemistry 13*, 5249–5256.
Venkatachalam, C. M., & Urry, D. W. (1983) *J. Comput. Chem. 4*, 461–469.
Wallace, B. A., & Ravikumar, K. (1988) *Science 241*, 182–187.
Weinstein, S., Wallace, B. A., Blout, E. R., Morrow, J. S., & Veatch, W. R. (1979) *Proc. Natl. Acad. Sci. U.S.A. 76*, 4230–4234.

Interplay of Phosphorylation and Dephosphorylation in Vision: Protein Phosphatases of Bovine Rod Outer Segments†

Charles Fowles and Muhammad Akhtar*
Department of Biochemistry, University of Southampton, Bassett Crescent East, Southampton SO9 3TU, England
Philip Cohen
Department of Biochemistry, University of Dundee, Medical Sciences Institute, Dundee, Tayside DD1 4HN, Scotland
Received May 1, 1989; Revised Manuscript Received July 11, 1989

ABSTRACT: Two types of protein phosphatases were identified in carefully prepared bovine rod outer segments (ROS). Extraction of the ROS with a medium-salt buffer solubilized protein phosphatase activity that was mainly type 2A, since it was active toward phosphorylase *a* in the absence of divalent cations, was not retained by heparin–Sepharose, dephosphorylated the α-subunit of phosphorylase kinase faster that the β-subunit, and was unaffected by inhibitor 2. Further extraction of the resulting membranes with a high-salt buffer solubilized additional phosphatase activity which was predominantly type 1, since it was retained by heparin–Sepharose and was blocked by inhibitor 2. The molecular mass of the type 2A phosphatase estimated by gel permeation chromatography on Superose 12 was 100 kDa, suggesting it may be the $2A_2$ form. Only the ROS type 2A phosphatase dephosphorylated opsin and rhodopsin efficiently. Concordant with this finding, the purified catalytic subunit of protein phosphatase 2A from rabbit skeletal muscle dephosphorylated opsin efficiently, while the type 1 catalytic subunit isolated from this tissue was inactive. Together, the results suggest that the ROS type 2A protein phosphatase plays an important role in regenerating rhodopsin from the various phosphorylated species in vivo. The activity of the enzyme per retina (~85 pmol of P_i released/min) is comparable to that of rhodopsin kinase (100 pmol of phosphate transferred/min).

Rhodopsin is the major protein present in the outer segments of rod cells of animal retinas. The activation of rhodopsin by light leads to the formation of a series of well-defined intermediates, and one of these, metarhodopsin II (hereafter referred to as Rho*),[1] plays a pivotal role in vision. The interaction of Rho* with transducin initiates a cascade of biochemical events leading to the transmission, and eventually to the registration, of the visual signal (Stryer, 1986). Thereafter, as for other physiological stimuli, the visual signal must be terminated. It is known that Rho* acts as a substrate for a specific kinase [rhodopsin kinase; Miller et al., 1977; see Kühn (1978) and references cited therein] present in the ROS (rod outer segments) that catalyzes the introduction of up to

†Supported by the Ulverscroft Foundation (M.A.) and the Medical Research Council, London, and Royal Society (P.C.). C.F. was the recipient of a postgraduate studentship from the SERC.

[1] Abbreviations: PMSF, phenylmethanesulfonyl chloride; ROS, rod outer segment(s); Rho*, metarhodopsin II.

0006-2960/89/0428-9385$01.50/0